Int J Clin Exp Med 2015;8(4):5150-5162
www.ijcem.com /ISSN:1940-5901/IJCEM0005923

Original Article

Improved antifungal activity of amphotericin B-loaded TPGS-b-(PCL-ran-PGA) nanoparticles

Xiaolong Tang[1,2*], Ronghong Jiao[3*], Chunmei Xie[4], Lifa Xu[1], Zhen Huo[1], Jingjing Dai[1], Yunyun Qian[1], Weiwen Xu[4], Wei Hou[2], Jiang Wang[1], Yong Liang[5]

[1]Stem Cell Engineering Research Center, School of Medical, Anhui University of Science & Technology, Huainan 232001, Anhui, P.R. China; [2]State Key Laboratory of Virology/Institute of Medical Virology, School of Basic Medical Sciences, Wuhan University, Wuhan 430071, P.R. China; [3]Department of Clinical Medical Laboratory, Shanghai Pudong New Area People's Hospital, Huai'an, Shanghai 201299, P.R. China; [4]School of Biotecl mology, Southern Medical University, Guangzhou 510515, China; [5]Clinical Laboratory, The Affiliated Huai'an Hospital of Xuzhou Medical College, Huai'an, Jiangsu 223002, P.R. China. [*]Equal contributors.

Received January 14, 2015; Accepted March 19, 2015; Epub April 15, 2015; Published April 30, 2015

Abstract: To develop amphotericin B-loaded biodegradable TPGS-b-(PCL-ran-PGA) nanoparticles (PLGA-TPGS-AMB NPs) for fungal infection treatment, PLGA-TPGS NPs and PLGA NPs were synthesized by a modified double emulsion method and characterized in terms of size and size distribution, morphology and zeta potential. Drug encapsulation efficiency, *in vitro* drug release, and *in vitro/vivo* tests against *Candida glabrata* were completed. The data showed that both of the two AMB-loaded NPs (PLGA-AMB NPs, PLGA-TPGS-AMB NPs) achieved significantly higher level of antifungal effects than water suspended AMB. In comparison with PLGA-AMB NPs, PLGA-TPGS-AMB NPs had a stronger protective effect against candidiasis and gained an advantage of prolonged antifungal efficacy. In conclusion, PLGA-TPGS-AMB NPs system significantly improves AMB bioavailability by increasing the aqueous dispersibility and improving the antifungal activity. And this would be an excellent choice for the antifungal treatment of the entrapped drug because of its low toxicity and higher effectiveness.

Keywords: Antifungal, *Candida glabrata*, amphotericin B, nanoparticle, TPGS-b-(PCL-ran-PGA)

Introduction

Amphotericin B (AMB) is a lipophilic polyene antifungal agent, which was initially secluded from a strain of *Streptomyces nodosus*. It is an amphoteric compound composed of a hydrophilic polyhydroxyl chain along one side and a lipophilic polyene hydrocarbon chain on the other [1]. AMB is sparingly soluble in water [2], and has a poor oral absorption. It has antibacterial activity against almost all fungi at the minimum inhibitory concentration (MIC) of 0.02-1 mg/L. AMB inhibits membrane enzymes like proton ATPase in fungal cells [2, 3] and Na^+/K^+-ATPase in mammalian cells and this inhibitory activity depletes cellular energy reserves and inhibits cell proliferative ability [4]. Moreover, the interaction of AMB with membrane sterol changes the fungal cell membrane permeability and results in an essential cellular substances such as potassium ions, nucleotides and amino acids leak, which in turn leads to cellular dysfunction and eventually to cell death [4, 5]. This is mainly valid to AMB for Candida, Cryptococcus, Histoplasma, yeast, dermatitis blastomycosis and Coccidioides. Broad antibacterial spectrum is in favor of the treatment of fungal infections via oral/intravenous administration. However, AMB has low bioavailability via oral administration because it is a highly hydrophobic weak base with a low aqueous solubility of approximately 1 ng/ml at pH 7 [1, 2].

Recently, drug delivery system (DDS) has received substantial attention in the field of drug development. In DDS, pharmacological techniques are used to control pharmacokinetic properties (absorption, distribution, metabolism, and excretion) and to improve the efficacy and safety of a drug. Copolymer formulations, such as nanoparticles and emulsion based car-

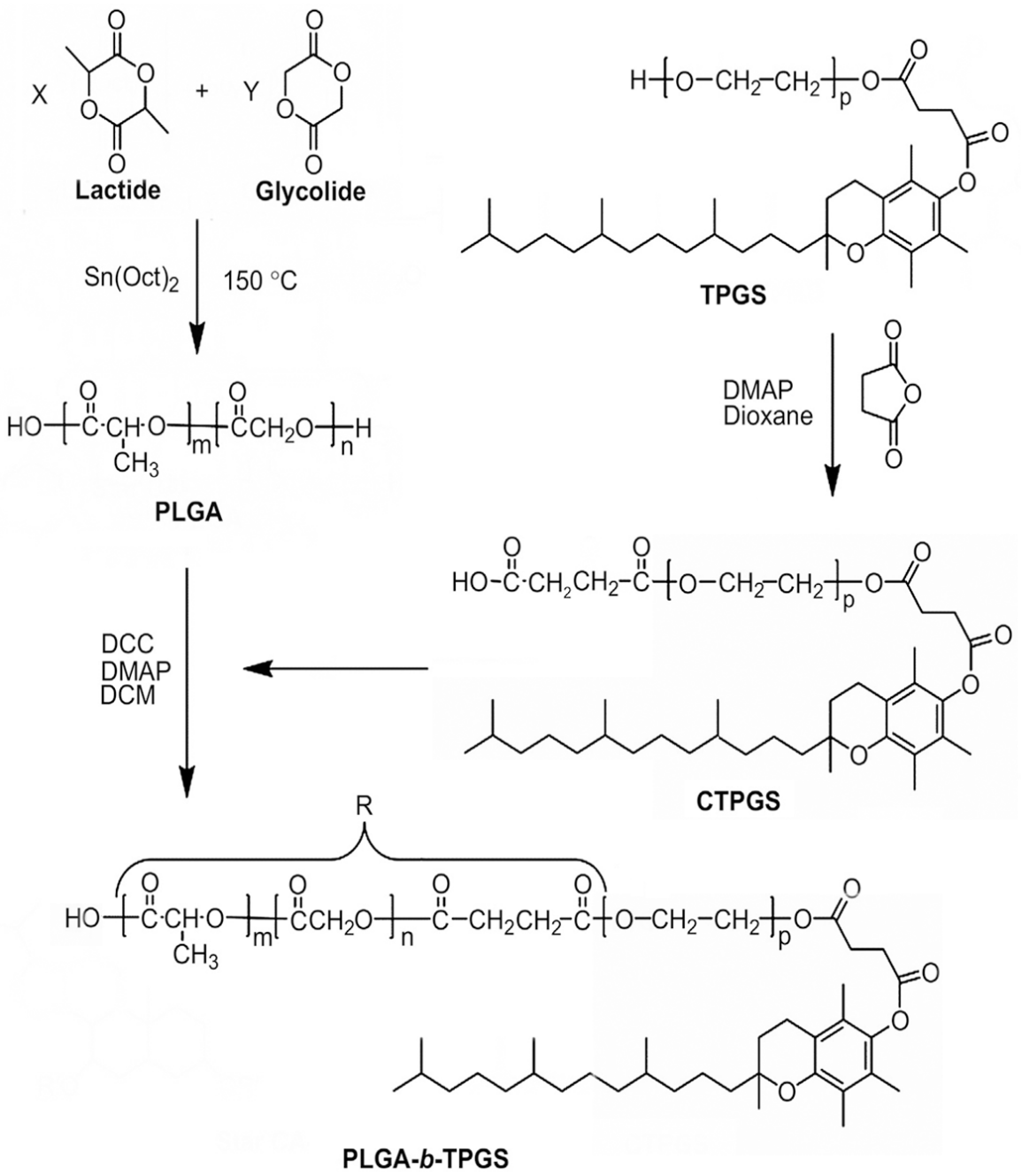

Figure 1. Schematic description of the synthesis of PLGA-TPGS random copolymer.

riers, are highly predictable and are now explored in numerous directions, and several products have already been made commercially available [6, 7]. Nanoparticle drug delivery systems such as biodegradable nanoparticles of poly (D, L-lactide-co-glycolide) (PLGA) have the advantages of increasing drug bioavailability, decreasing the fluctuation of drug concentration in blood, continuous drug release, gradual degradation in the body fluid, and variable routes of administration [8]. D-α-tocopheryl polyethylene glycol 1000 succinate-b-poly (ε-caprolactone-ran-glycolide) [TPGS-b-(PCL-ran-PGA), PLGA-TPGS] was a recently developed diblock copolymer. It demonstrated good biocompatibility and biodegradability [8]. Moreover, PLGA-TPGS NPs have higher drug encapsulation and cellular uptake, longer half

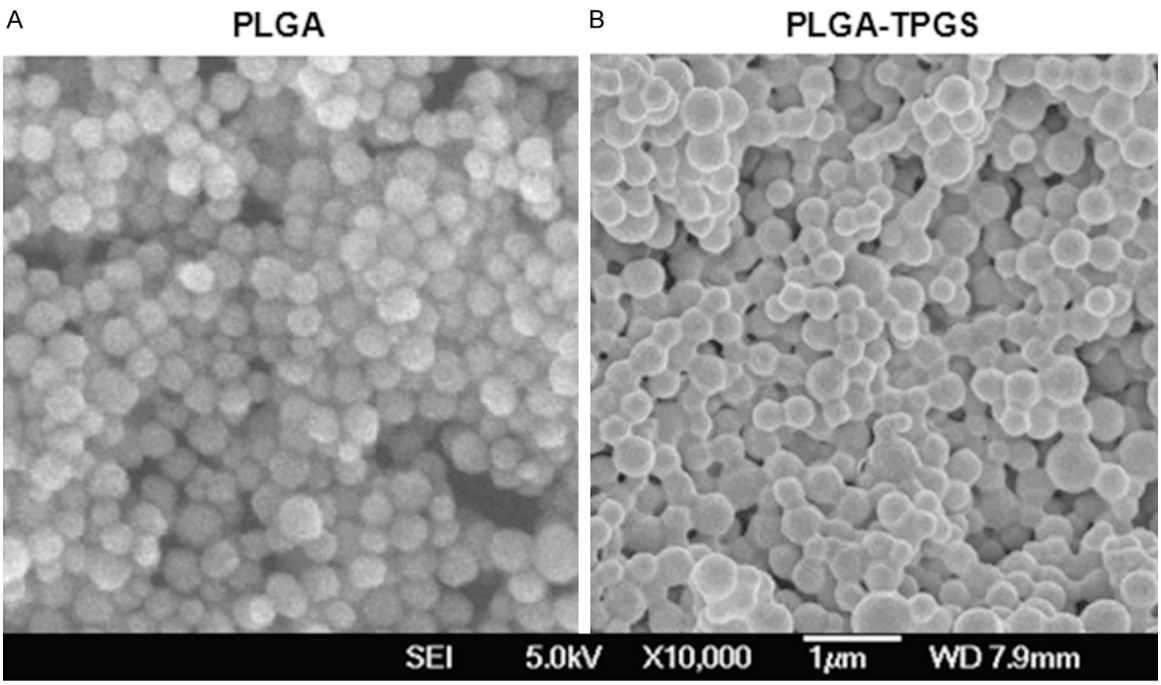

Figure 2. The physical properties of the star-shaped NPs. A, B: FESEM image of the PLGA and PLGA-TPGS NPs.

life and higher therapeutic effects of the formulated drug than PLGA NPs [8, 9].

Fungal infections have significantly contributed to the increasing morbidity and mortality of patients, especially immunocompromised patients [8, 9]. Therefore, this research aims to investigate the fungistatic and fungicidal effects of the AMB-loaded PLGA-TPGS NPs/PLGA NPs. Since *Candida spp.* represent one of the most common pathogenic yeasts blamed for life-threatening fungal infections [10], we chose *Candida glabrata* as (*C. glabrata*) a model fungus for the antimycotic capability test of drug-loaded NPs.

Materials and methods

Chemicals

D-α-tocopheryl polyethylene glycol 1000 succinate (TPGS, $C_{33}O_5H_{54}(CH_2CH_2O)_{23}$), D, L-lactide (3,6-dimethyl-1,4-dioxane-2,5-dione, $C_6H_8O_4$) with a purity greater than 99% and glycolide (1,4-Dioxane-2,5-dione, $C_4H_4O_4$) (purity > 99%) and poly (lactide-co-glycolide) (PLGA, *M*w approximately 25,000), Amphotericin B (AMB), Stannous octoate ($Sn(OOCC_7H_{15})_2$)and coumarin-6 were purchased from Sigma-Aldrich (St. Louis, MO, USA). PLGA-TPGS (*M*w approximately 23,000) copolymers were obtained from the Graduate School at Shenzhen, Tsinghua University. Acetonitrile and methanol were purchased from EM Science (Chrom AR, HPLC grade, Mallinckrodt Baker, USA). All other agents were of analytical grade or higher quality commercially available. Millipore water was prepared by a Milli-Q Plus System (Millipore Corporation, Breford, USA). *C. Glabrata* (*ATCC 90030)* was obtained from American Type Culture Collection (ATCC; Rockville, MD, USA).

Animals and fungal inoculation

20-22 g BALB/c mice of 6-8 weeks old were purchased from the animal house of Anhui Medical University (China). They had free access to food and water. The local Institute's Animal Ethics Committee approved all of the animal studies. The investigations conformed to the Guide for the Care and Use of Laboratory Animals published by the US National Institute of Health (NIH Published No. 85-23, revised 1996). Three days before the challenge, *Candida glabrata ATCC 90030* was subcultured daily in Sabouraud's dextrose broth. The subculture was pelleted and rinsed twice in sterile phosphate buffered saline (PBS) on the day of challenge. The final pellet was resuspended in PBS. The concentration of blasto-

Table 1. Characterization of AMB-loaded nanoparticles (*n* = 3)

Polymer	Particle size (nm)	PDI	ZP (mV)	LC (%)	EE (%)
PLGA-AMB	112.2 ± 4.3	0.265	-23.6 ± 0.5	8.11	76.01
PLGA-TPGS-AMB	122.7 ± 3.9	0.199	-19.5 ± 0.6	9.45	84.37

Note: PDI = polydispersity index, ZP = zeta potential, LC = loading content, EE = entrapment efficiency.

spores was counted with a hemacytometer and prepared for the following experiments.

Preparation of PLGA NPs and PLGA-TPGS NPs

PLGA-TPGS random copolymers were synthesized and characterized by a previously described method [8, 9]. 50 mg PLGA-TPGS random copolymer and 10 mg AMB were fully dissolved in 10 mL dichloromethane (DCM). The formed solution was poured into 50 mL 3% (w/v) polyvinyl alcohol solution under stirring. The mixture was sonicated for 10 min with pulses of 10 s on and 10 s off at 600 W output to form oil/water (O/W) emulsion. The organic solvent was then allowed to evaporate overnight under continuous magnetic stirring at 500 rpm. The reaction synthesis is schematically described in **Figure 1**. The hydroxyl end of TPGS served as initiator that selectively cleaves acyl oxygen chain of lactide or glycolide. The formation of the NPs and the encapsulation of AMB within the polymeric matrix were accomplished during the DCM evaporation process. The suspension was then dialyzed in a Regenerated Cellulose Dialysis Membrane (Spectra/Por 6, MWCO = 1000; Spectrum, Houston, Texas) bag with a molecular weight cut-off of 100 kDa to remove the emulsifier and unencapsulated AMB. The bag was put into a 3 L tank with nanopure water, at a ratio of 100:1 nanopure water to NPs, under gentle stirring for 8 h with the water changed every 4 h. The resulted suspension was freeze-dried at -50°C at a reduced pressure of 0.13 Pa for 48 h. The resulted PLGA-TPGS-AMB NPs were stored at -8°C for further analysis. PLGA-AMB NPs were synthesized following the same procedure.

Nanoparticles characterization and drug content and entrapment efficiency

The average size and size distribution of the prepared NPs were measured by Dynamic Light Scattering (Brookhaven Instruments Corporation, Holtsville, New York). 2 mg dried NPs were suspended in 200 μl ddH_2O before measurement. Zeta potential of the nanoparticles was determined by Zeta Plus zeta potential analyzer (Brookhaven Corporation). 10 μL suspended NPs were dropped onto platinum-coated copper grids and stained with 2% wt/vol phosphotungstic acid. The particles were then coated with a platinum layer using a JFC-1300 automatic fine platinum coater (JEOL) for 30 seconds in a vacuum. The surface morphologies of the NPs were observed by a field emission scanning electron microscopy using a JEOL JSM-6700F system (JEOL, Tokyo, Japan) operated at a 5.0 kV accelerating voltage.

To determine the contents of drug loading (LC) and entrapment efficiency (EE) of the AMB-loaded nanoparticles, a predetermined amount of nanoparticles was dissolved in 1 mL methylene dichloride under vigorous vortexing. The solution was transferred to 5 mL of mobile phase consisting of acetonitrile and deionized water (50:50, v/v). A nitrogen stream was introduced to evaporate the methylene dichloride for approximately 20 min, and then a clear solution was obtained for HPLC analysis (LC 1200, Agilent Technologies, Santa Clara, CA, USA). A reverse-phase C18 column (250 × 4.6 mm, 5 μm, Agilent Technologies, Santa Clara, CA, USA) was used at 25°C. The flow rate of the mobile phase was 0.5 mL/min. The column effluent was detected using a UV detector at λmax of 297 nm. The measurement was performed in triplicate. The LC and EE of the AMB-loaded nanoparticles were calculated by the following equations, respectively:

LC(%) = (Weight of AMB in the nanoparticles)/(Weight of the nanoparticles) × 100%;

EE(%) = (Weight of AMB in the nanoparticles)/(Weight of the feeding AMB) × 100%.

In vitro release of AMB from NPs

In vitro AMB release from nanoparticle formulations was performed as described previously [8, 9]. 10 mg of accurately weighted lyophilized nanoparticles was put into a centrifuge tube and redispersed in 15 mL PBS (containing 0.1% w/v Tween 80, pH 7.4). The tube was put into an orbital shaker water bath and vibrated at 150 rpm at 37°C. At certain time intervals, the tube

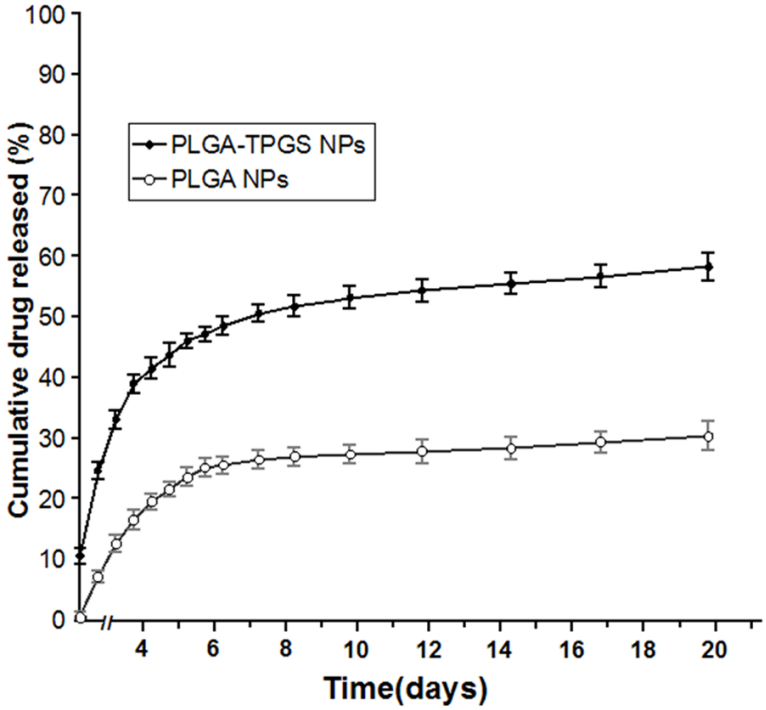

Figure 3. Cumulative release of AMB from PLGA-TPGS-AMB nanoparticles and PLGA-AMB nanoparticles (mean ± S.E.M., n = 5).

was taken out and centrifuged at 25,000 rpm for 15 min. The supernatant was then transferred to a glass test tube for HPLC analysis. The pellet was resuspended in 8 mL fresh PBS and placed back into the shaker bath for subsequent determination. The accumulative release of AMB from nanoparticles was plotted against time.

Cellular uptake of nanoparticles

In this research, coumarin 6 served as a model fluorescent molecule, which can be entrapped in the PLGA-TPGS nanoparticles for qualitative and quantitative studies on fungal cellular uptake. The cells were incubated with 250 μg/mL PLGA-TPGS-coumarin 6 nanoparticles at 37°C for 24 hrs, rinsed with cold PBS solution 3 times, and then fixed in methanol for 25 min before analysis by fluorescence microscopy.

Detection of apoptosis markers in C. glabrata

C. glabrata spores (1 × 10^6 spores/ml) were inoculated in RPMI 1640 medium at 37°C for 5 h with and without antifungal agents (PLGA-TPGS-AMB NPs, 10.0 μg/ml) and incubated for 12 h at 37°C with shaking (180 rpm). After incubation for 12 h, the *C. glabrata* cells were harvested and washed twice with PBS (pH 7.4). The cell wall was incubated with a lysing enzyme mixture (1.2 U of chitosanase, 1.3 U of chitinase, 1.5 U of lyticase, and 10 mg/ml lysing enzyme [Sigma]) for 5 h at 30°C. It was then digested and analyzed for the presence of apoptotic markers with Annexin V/PI; stains show the presence of apoptotic cells (green fluorescence) and necrotic cells (red fluorescence), as described by Madeo and Shirazi and Kontoyiannis [11]. The apoptotic and necrosis features in PLGA-TPGS-AMB NPs-treated *C. glabrata* cells were evaluated using annexin V-FITC and PI staining, respectively. Annexin V-FITC (Annexin V Apoptosis Detection Kit; BD Pharmingen) was used to detect phosphatidylserine that was translocated to the plasma membrane surface at the onset of apoptosis in *C. glabrata*. Five microliters of annexin V-FITC (50 μg/ml) and 5 μl of propidium iodide (PI) (200 μg/ml) were added to 1 ml of cell suspension, and the mixture was incubated for 20 min in the dark at RT [12].

Antifungal activity in vitro

Antifungal activity *in vivo* was tested by paper-plate technique. 10 μl of conidial suspension *C. glabrata* (1 × 10^5 spores/ml) was spread over the glucose agar plate. 5 mm diameter filter paper was made with a sterile borer and sterilized. Three pieces of sterile filter paper were placed on the solidified agar layer. Since AMB minimum inhibitory concentration (MIC) for *C. glabrata* was 0.2-1.0 μg/ml [13], 2.5/5/10/20/40 μl of PLGA-AMB NPs and PLGA-TPGS-AMB NPs at the concentration of 12.5 μg/ml and 10.6 μg/ml (equivalent to 1.0 μg/ml of AMB) respectively, and free AMB at 1.0 μg/mL emulsion were separately dropped onto the sterile filter paper. Petri plates were kept for 4 hours at room temperature and then were incubated at 28°C for 9 days. Digital photos of the cultures were taken after treatments were initi-

Table 2. Effect of free AMB and AMB-loaded nanoparticles on MIC against *C. Glabrata*

	MIC (μg/ml, n = 3)
Free AMB	0.87
PLGA-AMB NPs	0.96
PLGA-TPGS-AMB NPs	0.89
Empty PLGA nanoparticles	> 10.0
Empty PLGA-TPGS nanoparticles	> 10.0

Abbreviations: AMB, amphotericin B; MIC, minimum inhibitory concentration; PLGA, poly (d,l-lactide-co-glycolide); TPGS, d-α-tocopheryl polyethylene glycol 1000 succinate.

ated and the antifungal activity was evaluated every day. PLGA-TPGS-AMB NPs were compared against free AMB and PLGA-AMB NPs.

Animal studies

In vivo therapeutic efficacy of the prepared nanoparticles was tested by a described method [8, 9]. 60 BALB/c mice were challenged intravenously via the tail vein with 0.1 ml of *C. glabrata* cell suspension (1×10^7 cells/ml) in normal saline. All the treatments were intraperitoneally carried out 24 h after the challenge for the next 3 days and then randomly divided into 6 groups. All groups received the drug intravenously as follows: Groups I received PBS (1.0 mg/kg, pH = 7.4); group II received free AMB (1.0 mg/kg); group III received empty PLGA NPs (12.5 mg/kg, equivalent PLGA-AMB NPs 12.5 mg/kg); group IV received PLGA-AMB NPs (12.5 mg/kg, equivalent AMB 1.0 mg/kg); group V received empty PLGA NPs (10.6 mg/kg, equivalent PLGA-AMB NPs 10.6 mg/kg); group VI received PLGA-AMB NPs (10.6 mg/kg, equivalent AMB 1.0 mg/kg). All groups were treated as described above for 10 days starting from the 3rd day of infection. At the end of the experiment, the mice that survived were anesthetized and sacrificed. Then fungal colony forming units (CFU) in liver, kidney, spleen and right lung were determined, and the left lung tissue was embedded in paraffin and sectioned at 5 μm. Haematoxylin & eosin (HE) stain or Crystal violet stain and methylene blue stain were then performed.

Statistical analysis

Qualitative data such as AMB content loaded in PLGA-TPGS/PLGA NPs, biochemical data of PLGA-TPGS/PLGA NPs, and fungal burden in the mice lung tissue (CFU per gram of lung tissue) were expressed as mean ± S.E.M. Differences between paired groups were analyzed by Student's unpaired *t*-test. Probability values of $P < 0.05$ were considered to be statistically significant.

Results

NP characterization: morphology, size, zeta potential, encapsulation efficiency and release

Particle size and surface properties of the nanoparticles play a crucial role in drug release kinetics, cellular uptake behavior as well as in vivo pharmacokinetics and tissue distribution [14]. The physical properties of the PLGA-TPGS-AMB NPs and PLGA-AMB NPs were displayed in **Figure 2** and **Table 1**. The average hydrodynamic size of the PLGA-TPGS NPs and PLGA-TPGS-AMB NPs were approximately 110~120 nm and 120~130 nm in diameter respectively. These are within the size range for accumulating readily in tumor vasculature due to enhanced permeation and retention effects [15]. The particle size and size distribution of the PLGA-TPGS-AMB NPs were detected by dynamic light scattering (DLS) equipment, and the data were displayed in **Table 1**. According to PDI, ZP (mV), Particle Size (nm), LC (%) and EE (%) parameters, PLGA-TPGS Copolymer nanoparticles display perfect advantage for an efficient drug delivery vehicle. Zeta potential is an important predictor of dispersion stability of nanoparticles. A high absolute value of the zeta potential means high surface charge of the nanoparticles. As displayed in **Table 1** and **Figure 1**, the zeta potential of the PLGA-TPGS-AMB NPs was determined to be -19.5 mV, which was slightly higher than that of the PLGA-AMB NPs of zeta potential of about -23.6 mV. The negative surface charge of the nanoparticles may be due to the presence of ionized carboxyl groups of PLA and PGA segments [8, 9, 15].

It could also be deduced from **Table 1** that the contents of drug loading and entrapment efficiency of the PLGA-TPGS NPs were higher than those of the PLGA NPs, indicating the higher binding affinity between the PLGA-TPGS and hydrophobic AMB. Moreover, the drug loading content of AMB in the PLGA-TPGS NPs could reach approximately 9.5%, which is ideal for an efficient drug delivery vehicle. After redispersion in PBS, the mean size and size distribution of the AMB-loaded nanoparticles were almost

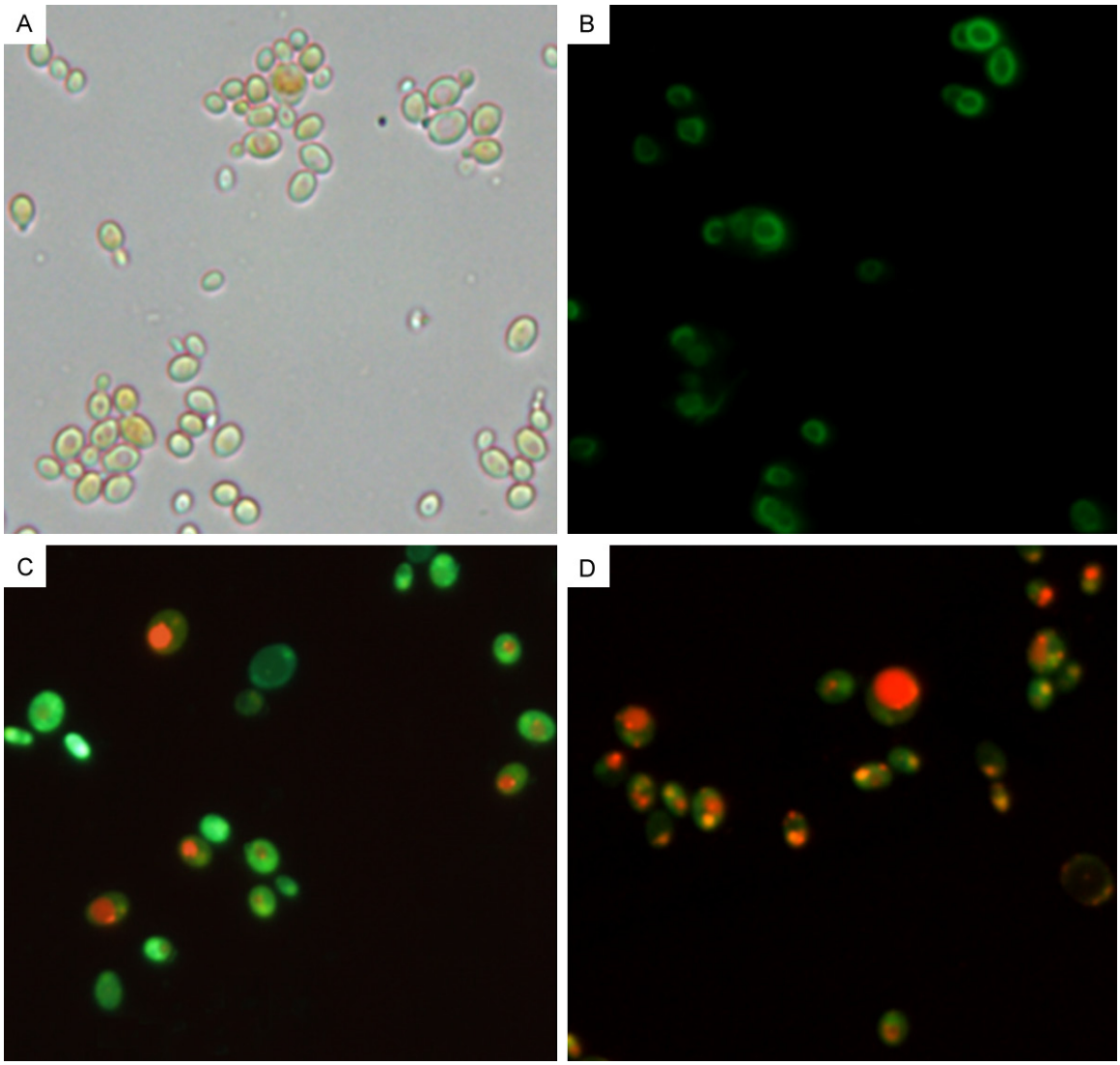

Figure 4. Representative photomicrographs of AMB-treated *C. Glabrata* cells using a fluorescence microscope. A: Bright-field images of *C. Glabrata*. B: *C. Glabrata* cellular uptake and fluorescence image of the coumarin 6-loaded nanoparticles after 24 h incubation with the PLGA-TPGS-coumarin 6 nanoparticles. The cellular uptake was visualized by overlaying images obtained by EGFP filter. C: Effects of 24 h treatment with AMB on the activity of *C. Glabrata* as confirmed using Annexin V/PI. D: Effects of 48 h treatment with AMB on the activity of *C. Glabrata* as confirmed using Annexin V/PI. Annexin V/PI stains show the presence of apoptotic cells (green fluorescence) and necrotic cells (red fluorescence). The experiments were performed in triplicate and repeated three times. Magnification × 400.

unchanged during the 3 months of follow-up. This suggested that the AMB-loaded nanoparticles had good stability and redispersion ability.

In vitro drug release

The *in vitro* drug release profiles of the freshly prepared AMB-loaded nanoparticles in PBS (containing 0.1% *w/v* Tween 80, pH 7.4) in the first 22 days was studied and displayed in **Figure 3**. Tween 80 was applied to improve the solubility of AMB in the PBS and to prevent the adhesion of AMB onto the tube wall [16]. The AMB release from the PLGA-TPGS NPs and PLGA NPs displayed an initial burst of 47.38% and 33.35% respectively in the first 5 days. It was followed by a second slow-release phase sustained for up to 22 days, which was predominantly attributed to the diffusion of the drug. After 22 days, the accumulative AMB release of nanoparticles reached 45%~65%. The accumulative AMB release in the first 22 days was found in the following order: PLGA-TPGS

Table 3. The ratio of survived mice and colony-forming units (CFU) in different organs of infected-mice

	Log CFU gram tissue (n = 3)				Survival ratio[a] (%, n = 20)
	Lung	Liver	Kidney	Spleen	
Control	3.51 ± 0.53	3.13 ± 0.36	3.91 ± 0.46	2.22 ± 0.65	0.0
PBS	3.38 ± 0.46	3.10 ± 0.42	3.89 ± 0.52	2.11 ± 0.48	0.0
Free AMB	2.31 ± 0.03*	1.11 ± 0.13*	1.12 ± 0.29*	1.20 ± 0.24*	30.0
PLGA	3.40 ± 0.32	3.15 ± 0.71	3.90 ± 0.81	2.21 ± 0.46	0.0
PLGA-AMB	1.08 ± 0.04*	1.05 ± 0.03*	Nil**	Nil**	45.0
PLGA-TPGS	3.44 ± 0.47	3.11 ± 0.75	3.87 ± 0.88	2.19 ± 0.91	0.0
PLGA-TPGS-AMB	1.02 ± 0.03*	1.01 ± 0.02*	Nil**	Nil**	85.0

The values are expressed as means ± S.E.M. from three separate experiments. Analysis of variance of one-way classification between the treatment means was heterogeneous, and the *t*-test values (two-tailed) were significant. *$P < 0.05$, **$P < 0.001$. [a]: Percentage of survival 10 days after the therapy (n = 20).

nanoparticles > PLGA nanoparticles, indicating that the PLA-TPGS copolymer was capable of displaying faster drug release than the PLGA nanoparticles when the copolymers had the same molecular weight.

In vitro antifungal activity

To evaluate the antifungal activity of the AMB-loaded nanoparticles, the minimum inhibitory concentration of free AMB, AMB-loaded nanoparticles, empty PLGA and PLGA-TPGS copolymer nanoparticles were tested with *C. glabrata.* As shown in **Table 2**, the minimum inhibitory concentration of the AMB-loaded nanoparticles was similar to that of free AMB, while the empty polymeric nanoparticles had a much higher minimum inhibitory concentration value, indicating that AMB-loaded nanoparticles have an antifungal potential similar to that of free AMB. However, the PLGA, PLGA-TPGS copolymer did not affect the antifungal activity of the polymeric nanoparticles.

Cellular uptake of fluorescent PLGA-TPGS nanoparticles and antifungal activity

The therapeutic effects of the drug-loaded polymeric nanoparticles were dependent on internalization and sustained retention of the nanoparticles by fungal cells [17]. The in vitro studies were capable of providing some circumstantial evidence to show the advantages of the nanoparticle formulation compared with the free drug. Coumarin-6 served as a fluorescent probe in an attempt to represent the drug in the nanoparticles for visualization and quantitative analysis of cellular uptake of the nanoparticles [8, 9]. **Figure4A** and **4B** respectively showed the images of *C. glabrata* cells in light and fluorescence microscopy after 24 h incubation with the PLGA-TPGS-coumarin six nanoparticles at the concentration of 250 μg/mL. It could be seen from this figure (**Figure 4B**) that the PLGA-TPGS-coumarin 6 nanoparticles (green) were closely located around the fungi, indicating that the nanoparticles show high *affinity to C. glabrata* cells.

To investigate whether the drug can actually induce apoptosis and necrosis in *C. glabrata* cells, the apoptotic and necrosis features in PLGA-TPGS-AMB NPs-treated *C. glabrata* cells using annexin V-FITC and PI double-staining method were evaluated. Apoptotic cells are stained with annexin V-FITC, whereas PI accumulates in the nuclei of necrotic cells via membrane permeabilization [18]. Following PLGA-TPGS-AMB NPs (5.0 μg/ml, equivalent AMB 0.5 μg/ml) exposure at 37°C for 24 h, about 96% of the cells were stained with annexin V-FITC, while only 25% to 43% of the cells were stained with PI. However, when PLGA-TPGS-AMB NPs treatment was extended to 48 h, almost of all the cells were stained with annexin V-FITC, and only 85% to 95% of the cells were PI positive as shown in **Figure 4C** and **4D**. These results suggested that PLGA-TPGS-AMB induced apoptosis in *C. glabrata* cells.

Therapeutic efficacy of AMB-loaded nanospheres

The treatment of *C. glabrata*-infected mice with AMB-loaded nanospheres as compared with control animals showed a significant reduction in CFU values in evaluated organs especially in kidney and spleen (**Table 3**). It was discovered

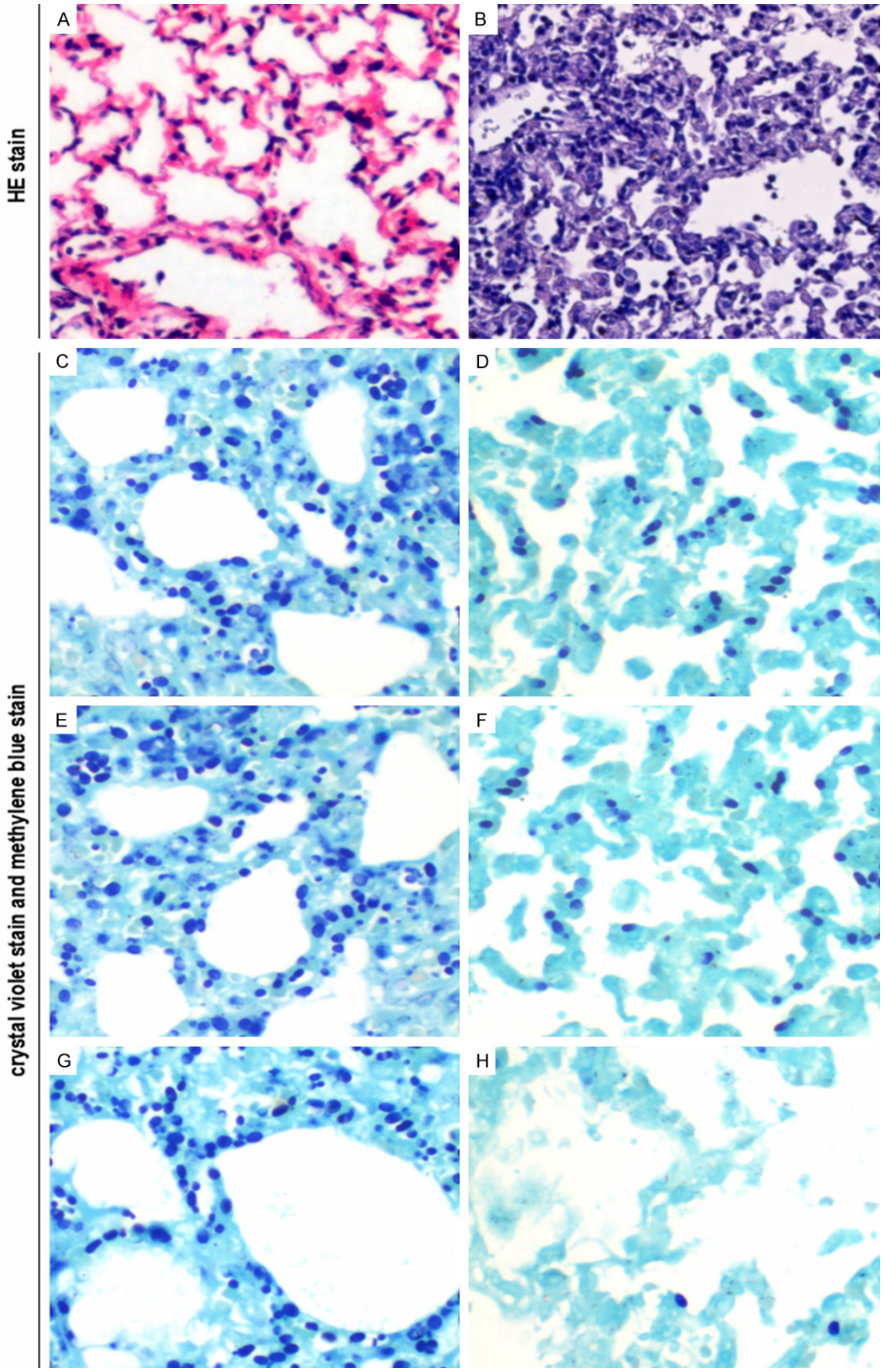
HE stain
crystal violet stain and methylene blue stain
A
B
C
D
E
F
G
H

Figure 5. Photomicrographs of infected lung tissue section of *C. glabrata.* A: Normal healthy lung section stained with H&E. B, C: Infected lung tissue section of *C. glabrata* was stained with H&E and Crystal violet showing pulmonary interstitial edema, with numerous intracellular and extracellular circular to oval, elongated, thin-walled yeast-like moniliform hyphal organisms. D, F: Infected lung tissue treated with free AMB (1.0 μg/mg) and PLGA-AMB NPs (12.5 μg/mg, equivalent AMB 1.0 μg/mg), showing that pulmonary interstitial edema significantly reduced pulmonary interstitial edema, and fungal cells proliferation were significantly inhibited. E, G: Infected lung tissue treated with empty PLGA NPs and PLGA-TPGS NPs vector showing that changes in the lung tissue were the same with that of the infected-control group. H: Infected lung section treated with PLGA-TPGS-AMB NPs (10.3 μg/mg, equivalent AMB 1.0 μg/mg), it shows that lung tissue was free from edema and damage with much lower level of fungal spores after the PLGA-TPGS-AMB treatment. Magnification × 400.

that the mortality of *C. glabrata*-infected mice used as control (without AMB administrated) was 100% after 10 days, whereas mice treated with free AMB and AMB-loaded nanospheres showed increase in survival rate of 40.0 and 85.0%, respectively. One of the reasons for the differences in the antifungal potencies and toxicities among free AMB and prepared AMB formulations could be due to high stability of AMB-loaded nanoparticles [8, 9].

Interestingly, data of the fungal burden of the different organs analyzed showed that free AMB would favorably reduce the amount of bacteria in the lungs, kidneys and livers. However, its therapeutic effect was significantly weaker than that of PLGA-AMB and PLGA-TPGS-AMB (**Table 3**). The kidneys and spleens of PLGA-AMB and PLGA-TPGS-AMB groups had no fungal growths. Also the fungal amount in the lungs and livers were effectively suppressed compared with the control group.

Lung histological analysis

As shown in **Figure 5**, lung tissue structures in the normal group were well defined without discernible damage or edema, and the trachea and blood vessels were not infiltrated peripherally by inflammatory cells (**Figure 5A**). However, lung tissue and bronchial structures in the *C. glabrata*-infected model mice were disturbed by internal hemorrhage and edema; the bronchial and vascular walls were thickened and infiltrated by a considerable number of inflammatory cells (**Figure 5B** and **5C**). Lung tissue was free from edema and damage after 10 days of the PLGA-TPGS-AMB treatment (**Figure 5H**). In the PLGA NPs and PLGA-TPGS NPs treatment groups, there was marked irregular architecture and inflammatory cell infiltration. As fungal infected control groups, there was a notable histological changes; the bronchial and vascular walls were thickened, and numerous fungal cells infiltrated the lung tissue (**Figure 5E** and **5G**). Nevertheless, the histological results of the free AMB group and PLGA-AMB group generally improved relative to those of the *C. glabrata* infected models, although lung tissues in the two groups showed histological changes with occasional inflammatory cell infiltration similar to that seen in the normal group. They also showed significantly reduced pulmonary interstitial edema (**Figure 5D** and **5F**).

Discussion

Pulmonary fungal infections are serious life-threatening diseases. To improve the treatment of pulmonary infections, several antifungal agents including formulations of echinocandins, pyrimidines and polyenes were used. Amphotericin B (AMB) is a kind of systemic antifungal polyene holding broad-anti-fungal spectrum, and has a good antibacterial effect for a variety of deep fungal infections such as Cryptococcus neoformans, Candida albicans, Coccidioides immitis, Histoplasma capsulatum fungus, dermatitis blastomycosis, Schenck Sporothrix, Aspergillus, and Mucor [2, 6, 19]. Having the broad antifungal spectrum, AMB has become the most important antifungal agents [1, 20]. However, safety remains an important consideration. AMB has common adverse reactions of the digestive system, serious toxicity to the kidneys, and even causes leukopenia and liver damage [15, 21]. The goal of this study is to determine whether a novel nanoparticle delivery platform for AMB is less disruptive to lung epithelium than existing formulations of AMB without affecting the efficacy of AMB. We hypothesized that AMB would cause minimal damage to the lung when formulated within the nanoparticles (NPs).

The stability of nanocarriers that will minimize the release of drug in the blood circulatory system plays a major role in determining the rate

and extent of absorption of drugs from different tissues. Many researchers have found that the biodegradable PLA-TPGS polymerizer could enhance drug stability of decreased drug non-specific toxicity, which may be an ideal carrier for AMB [19, 22]. As shown by FESEM, all the prepared particles were homogeneously spherical and smooth (**Figure 1**). **Table 1** summarizes the size, polydispersity index, zeta potential, and EE for different NPs. Size measured via dynamic light scattering reported PLGA-TPGS-AMB NPs at 118-127 nm and PLGA-AMB NPs at 107-117 nm, respectively. The polydispersity index ranged from 105-130 nm, which is very conducive for cellar absorption and internalization [8, 9, 23]. The respective EE% of PLGA-TPGS-AMB NPs and PLGA-AMB NPs were 84.37% and of 76.01% (**Table 1**). This confirmed the truth that the drug EE% of PLGA-TPGS is higher than that of PLGA. The surface charge of the NPs is an important physicochemical parameter that can influence their stability in suspension, which can also influence the interaction between the NPs and the cell membrane *in vivo*. In the case of a combined electrostatic and steric stabilization, a minimum zeta potential of ± 20 mV is desirable [22, 23]. As displayed in **Table 1**, all formulations showed nearly similar zeta potential of-22 mV. Specifically, the zeta potential of PLGA-TPGS-AMB was just in the range of ± 20 mV. AMB release from PLGA-TPGS NPs suspended in PBS was biphasic, with an initial jump of 65% in 15 days, followed by a steady release over 10 days (**Figure 2**). The initial jump was attributed to the presence of the drug released near the particle surface. Thereafter, the drug was released by a combination of diffusion and particle degradation [13, 24]. Over this period, AMB was consequently administered with increased efficacy. The D-α-tocopheryl polyethylene glycol 1000 succinate (TPGS) has amphiphilic structure comprising of hydrophilic polar head group (tocopherol succinate). Its bulky structure and large surface area make it an excellent solubilizer, emulsifier, and bioavailability enhancer of hydrophobic drugs [19, 21]. Cellular uptake combined with the AMB release in the vicinity of the cell surface leads to a quicker internalization of AMB; AMB was efficiently internalized, and then gradually released from the NPs in a sustained manner [25]. Our results further suggested that the PLGA-TPGS NPs was an excellent hydrophobic drug polymer carrier.

To investigate whether the drug can effectively induce apoptosis and necrosis of *C. glabrata* cells, the apoptotic and necrosis features in PLGA-TPGS-AMB NPs-treated *C. glabrata* cells were evaluated using annexin V-FITC and PI double-staining method. Apoptotic cells were stained with annexin V-FITC, whereas PI accumulated in the nuclei of necrotic cells via membrane permeabilization [25]. Following PLGA-TPGS-AMB NPs (5.0 μg/ml, equivalent AMB 0.5 μg/ml) exposure at 37°C for 24 h, about 96% of the cells were stained with annexin V-FITC, while only 25% to 43% of the cells were stained with PI. However, when PLGA-TPGS-AMB NPs treatment was extended to 48 h, almost all the cells were stained with annexin V-FITC, and only 85% to 95% of the cells were PI positive as shown in **Figure 3C** and **3D**. These results suggested that the PLGA-TPGS nanoparticles *shows high affinity to C. glabrata* cells and PLGA-TPGS-AMB NPs could effectively induce apoptosis and necrosis of *C. glabrata* cells. Therefore, our data further confirms that the PLGA-TPGS-AMB NPs formulation has more therapeutic advantages compared with the free AMB and PLGA- AMB NPs *in vitro*.

Besides the *in vitro* results, the antifungal efficacy of the free-AMB, PLGA-TPGS-AMB-NPs and PLGA-AMB-NPs formulation was further observed *in vivo*. **Table 3** shows the CFU/g lung tissues from mice treated with different AMB formulation were respectively. The free-AMB, PLGA-TPGS-AMB NPs, and PLGA-AMB NPs groups showed a marked decrease on day 5 after being administered in the lung CFU compared with the PBS group. Moreover, PLGA-TPGS-AMB NPs showed more potency in reducing fungal burden in the lungs campared with free AMB and PLGA-AMB NPs groups. The survival ratio of PLGA-TPGS-AMB NPs group was higher than the PLGA-AMB NPs, free AMB, and control groups (**Table 3**), and the histopathology corroborated the antifungal efficacy of free-AMB, PLGA-TPGS-AMB NPs and PLGA-AMB NPs. Hematoxylin & eosin (HE) stain confirmed the pathological changes observed in the *C.glabrata* infected group with inflammatory infiltration, swelling of alveolar wall capillary vessel, pulmonary interstitial edema, fungal cells proliferation and infiltration. PLGA-TPGS NPs and PLGA NPs did not alleviate these pathological changes in the lungs, nor inhibit the proliferation of fungi (**Figure 5** and **Table 3**).

However, those lesions were revealed in the mice treated with free-AMB and PLGA-AMB NPs, but those treated with PLGA-AMB NPs showed almost no detectable lesions.

Conclusions

The developed PLGA-TPGS-AMB NPs gave an appropriate particle size, extended drug release, and zeta potential. The *in vitro/vivo* results of *C. glabrata* in the present study showed significantly higher level of antifungal effects than water suspended AMB. This indicated that the developed PLGA-TPGS-AMB NPs delivery system may be more appropriate for the treatment of fungal infection because its efficacy and balanced toxicity. We envisage that it might probably serve as a useful novel antifungal drug delivery system for the treatment of patients with fungal infections in the future. Further experiments on PLGA-TPGS-AMB NPs including its specific action mechanism, toxicity, as well as costs of consumption will be conducted to reveal more of their characteristics.

Acknowledgements

The authors are grateful for the Open Research Fund Program of the State Key Laboratory of Virology of China (No. 2014KF004), the science and technology supporting fund in Huai'an (No. HAS2013010), the startup funds for science research from Huai'an Second People's Hospital (No. YK201217), the National High Technology Research and Development Program (863 Program) (No. 2011AA02A111), and 2011 Infectious Disease Prevention and Control Technology major project (No. 2012-ZX10004903).

Disclosure of conflict of interest

None.

Address correspondence to: Jiang Wang, Stem cell Engineering Research Center, School of Medicine, Anhui University of Science & Technology, Huainan, Anhui 232001, P.R. China. E-mail: txljd2006@126.com; Yong Liang, Clinical Laboratory, The Affiliated Huai'an Hospital of Xuzhou Medical College, Huai'an 223002, China. E-mail: liangyong20142015@163.com

References

[1] Stephens N, Rawlings B and Caffrey P. Streptomyces nodosus host strains optimized for polyene glycosylation engineering. Biosci Biotechnol Biochem 2012; 76: 384-387.

[2] Storm G and van Etten E. Biopharmaceutical aspects of lipid formulations of amphotericin B. Eur J Clin Microbiol Infect Dis 1997; 16: 64-73.

[3] Surarit R and Shepherd MG. The effects of azole and polyene antifungals on the plasma membrane enzymes of Candida albicans. J Med Vet Mycol 1987; 25: 403-413.

[4] Stratford M, Nebe-von-Caron G, Steels H, Novodvorska M, Ueckert J and Archer DB. Weak-acid preservatives: pH and proton movements in the yeast Saccharomyces cerevisiae. Int J Food Microbiol 2013; 161: 164-171.

[5] Perez-Schindler J, Summermatter S, Salatino S, Zorzato F, Beer M, Balwierz PJ, van Nimwegen E, Feige JN, Auwerx J and Handschin C. The corepressor NCoR1 antagonizes PGC-1alpha and estrogen-related receptor alpha in the regulation of skeletal muscle function and oxidative metabolism. Mol Cell Biol 2012; 32: 4913-4924.

[6] Bhattacharyya A and Bajpai M. Oral bioavailability and stability study of a self-emulsifying drug delivery system (SEDDS) of amphotericin B. Curr Drug Deliv 2013; 10: 542-547.

[7] Zhou W, Zhou Y, Wu J, Liu Z, Zhao H, Liu J and Ding J. Aptamer-nanoparticle bioconjugates enhance intracellular delivery of vinorelbine to breast cancer cells. J Drug Target 2014; 22: 57-66.

[8] Tang X, Cai S, Zhang R, Liu P, Chen H, Zheng Y and Sun L. Paclitaxel-loaded nanoparticles of star-shaped cholic acid-core PLA-TPGS copolymer for breast cancer treatment. Nanoscale Res Lett 2013; 8: 420.

[9] Mu L and Feng SS. PLGA/TPGS nanoparticles for controlled release of paclitaxel: effects of the emulsifier and drug loading ratio. Pharm Res 2003; 20: 1864-1872.

[10] Sato M, Ohshima T, Maeda N and Ohkubo C. Inhibitory effect of coated mannan against the adhesion of Candida biofilms to denture base resin. Dent Mater J 2013; 32: 355-360.

[11] Wang H, Leavitt L, Ramaswamy R and Rapraeger AC. Interaction of syndecan and alpha6beta4 integrin cytoplasmic domains: regulation of ErbB2-mediated integrin activation. J Biol Chem 2010; 285: 13569-13579.

[12] Cho J, Hwang IS, Choi H, Hwang JH, Hwang JS and Lee DG. The novel biological action of antimicrobial peptides via apoptosis induction. J Microbiol Biotechnol 2012; 22: 1457-1466.

[13] Pfaller MA, Hata K, Jones RN, Messer SA, Moet GJ and Castanheira M. In vitro activity of a novel broad-spectrum antifungal, E1210, tested against Candida spp. as determined by CLSI broth microdilution method. Diagn Microbiol Infect Dis 2011; 71: 167-170.

[14] Kiriyama A, Iga K and Shibata N. Availability of polymeric nanoparticles for specific enhanced and targeted drug delivery. Ther Deliv 2013; 4: 1261-1278.
[15] Verma RK, Pandya S and Misra A. Loading and release of amphotericin-B from biodegradable poly (lactic-co-glycolic acid) nanoparticles. J Biomed Nanotechnol 2011; 7: 118-120.
[16] Van de Ven H, Paulussen C, Feijens PB, Matheeussen A, Rombaut P, Kayaert P, Van den Mooter G, Weyenberg W, Cos P, Maes L and Ludwig A. PLGA nanoparticles and nanosuspensions with amphotericin B: Potent in vitro and in vivo alternatives to Fungizone and AmBisome. J Control Release 2012; 161: 795-803.
[17] Jiang L, Li X, Liu L and Zhang Q. Thiolated chitosan-modified PLA-PCL-TPGS nanoparticles for oral chemotherapy of lung cancer. Nanoscale Res Lett 2013; 8: 66.
[18] Hwang IS, Lee J, Hwang JH, Kim KJ and Lee DG. Silver nanoparticles induce apoptotic cell death in Candida albicans through the increase of hydroxyl radicals. FEBS J 2012; 279: 1327-1338.
[19] Yap WT, Song WK, Chauhan N, Scalise PN, Agarwal R, Miller SD and Shea LD. Quantification of particle-conjugated or particle-encapsulated peptides on interfering reagent backgrounds. Biotechniques 2014; 57: 39-44.
[20] Chakraborty KK and Naik SR. Therapeutic and hemolytic evaluation of in-situ liposomal preparation containing amphotericin-beta complexed with different chemically modified beta-cyclodextrins. J Pharm Pharm Sci 2003; 6: 231-237.
[21] Turk CT, Oz UC, Serim TM and Hascicek C. Formulation and optimization of nonionic surfactants emulsified nimesulide-loaded PLGA-based nanoparticles by design of experiments. AAPS PharmSciTech 2014; 15: 161-176.
[22] Vrignaud S, Hureaux J, Wack S, Benoit JP and Saulnier P. Design, optimization and in vitro evaluation of reverse micelle-loaded lipid nanocarriers containing erlotinib hydrochloride. Int J Pharm 2012; 436: 194-200.
[23] Silva AC, Kumar A, Wild W, Ferreira D, Santos D and Forbes B. Long-term stability, biocompatibility and oral delivery potential of risperidone-loaded solid lipid nanoparticles. Int J Pharm 2012; 436: 798-805.
[24] Li H, Wang P, Liu Q, Cheng X, Zhou Y and Xiao Y. Cell cycle arrest and cell apoptosis induced by Equisetum hyemale extract in murine leukemia L1210 cells. J Ethnopharmacol 2012; 144: 322-327.
[25] Silva AE, Barratt G, Cheron M and Egito ES. Development of oil-in-water microemulsions for the oral delivery of amphotericin B. Int J Pharm 2013; 454: 641-648.